Development of a Coupled-Channels Optical Model Code "OPTMAN" and a Global CC Potential as a Base for High Energy Nuclear Data Evaluation

Efrem Sh. Soukhovitski[1], and Satoshi Chiba[2]
[1] *Joint Institute for Energy and Nuclear Research Sosny, Academician A.K. Krasin 99, 220109, Minsk-Sosny, Belarus*
[2] *Japan Atomic Energy Research Institute, Tokai-mura, Naka-gun,Ibaraki-ken,319-1195, Japan*
e-mail: esukhov@sosny.bas-net.by

Coupled-channels optical model code "OPTMAN" with coupling built on wave functions of the Soft-rotator nuclear Hamiltonian was completely modernized to be a base for high energy nuclear data evaluation. It was used to analyze experimental nucleon optical interaction data with A=24-122 mass nuclides. We found that all the available experimental data (total cross sections, angular distributions of elastically and inelastically scattered nucleons and reaction cross sections) for these nuclides can be described with good accuracy using smooth A-mass dependencies of optical potential values while imaginary volume potential geometry was considered to be equal real potential one, with individual properties of the nuclides accounted by individuality of the nuclear Hamiltonian parameters, Fermi energies and deformations.

1. Introduction

For more than twenty years an original coupled-channels optical model code OPTMAN has been developed at Joint Institute of Energy and Nuclear Research to investigate neutron-nucleus interaction mechanisms and as a basic tool for evaluation of reactor oriented nuclear data. Results of such activities for, e.g., ^{235}U, ^{239}Pu, ^{236}U, ^{233} U, ^{238}Pu etc., were included in evaluated Nuclear Data Library BROND[1] of former Soviet Union. Except for the standard rigid rotator and harmonic vibrator coupling scheme encoded in widely-used JUPITER[2] and ECIS[3] codes, level-coupling schemes based on a non-axial soft-rotator model are possible for the even-even nuclei in OPTMAN. This allows account of stretching of soft nuclei by rotations, which results in change of equilibrium deformations for excited collective states compared with that of the ground state. This is a critical point for reliable predictions[4, 5, 6] based on the coupled-channels method.

In 1997 in the framework of ISTC Project CIS-03-95, Financial Party of which was Japan, OPTMAN code was installed at Nuclear Data Center of Japan Atomic Energy Research Institute (JAERI) and an active collaboration started. After that time, many new options were added to the code following demands from a broad range of applications: power reactors, shielding design, radiotherapy, transmutations of nuclear wastes and nucleosynthesis.

Here we describe the activity performed under the Project Agreement B-521 of the International Science and Technology Center (Moscow). The work was requested by JAERI and is the result of a close cooperation between scientists from Joint Institute of Energy and Nuclear Research and JAERI.

2. Soft-Rotator Nuclear Model Coupled Channels and Optical Potential Form for Global Search

Soft-rotator nuclear model and its application to coupled-channels optical model calculations is described elsewhere[7]. We assume that the low-lying excited states observed in even-even non-spherical nuclei can be described as a combination of rotation, β-quadrupole and octupole vibrations, and γ-quadrupole vibration. Instant nuclear shapes that correspond to such excitations can be presented [8, 9] in a body fixed system:

$$R(\theta',\varphi') \;=\; R_0\left\{1+\sum_{\lambda=2,3,4\mu=even}\beta_{\lambda\mu}Y_{\lambda\mu}(\theta',\varphi')\right\}.$$

The Hamiltonian $\hat{H}$ of the soft-rotator model consists of the kinetic energy term for the rotation of the non-axial nuclei with quadrupole, hexadecapole and octupole deformations, the β_2-, γ-quadrupole and octupole vibrations, and the vibrational potentials ignoring a coupling between the three vibration modes [5]:

$$\hat{H}=\frac{\hbar^2}{2B_2}\left\{\hat{T}_{\beta_2}+\frac{1}{\beta_2^2}\hat{T}_{\gamma}\right\}+\frac{\hbar^2}{2}\hat{T}_r+\frac{\hbar^2}{2B_3}\hat{T}_{\beta_3}+\frac{\beta_{20}^4}{\beta_2^2}V(\gamma)+V(\beta_2)+V(\beta_3),$$

where

$$\begin{aligned}\hat{T}_{\beta_2} &= -\frac{1}{\beta_2^4}\frac{\partial}{\partial\beta_2}\left(\beta_2^4\frac{\partial}{\partial\beta_2}\right),\\ \hat{T}_{\gamma} &= -\frac{1}{\sin 3\gamma}\frac{\partial}{\partial\gamma}\left(\sin 3\gamma\frac{\partial}{\partial\gamma}\right),\\ \hat{T}_{\beta_3} &= -\frac{1}{\beta_3^3}\frac{\partial}{\partial\beta_3}\left(\beta_3^3\frac{\partial}{\partial\beta_3}\right).\end{aligned}$$

The symbol $\hat{T}_r$ denotes the operator of deformed nuclear rotational energy expressed in terms of the angular momentum operator and principal moments of inertia

$$\hat{T}_r=\sum_{i=1}^{3}\frac{\hat{I}_i^2}{J_i} \;=\; \sum_{i=1}^{3}\frac{\hat{I}_i^2}{J_i^{(2)}+J_i^{(3)}+J_i^{(4)}}. \qquad (1)$$

Here, $J_i^{(\lambda)}$ stands for the principal moments of inertia in the direction of the i-th axis in the body-fixed system due to quadrupole, octupole and hexadecapole deformations depending on λ=2, 3 and 4 respectively. The symbol $\hat{I}_i$ denotes the projection of the angular momentum operator on the i-th axis of the body-fixed coordinate, β_{20} -the quadrupole equilibrium deformation parameter at the ground state (G.S.) and B_λ -the mass parameter for multipolarity of λ. The eigenfunctions Ω of the collective energy operator are defined in the space of six dynamical variables: $0\le\beta_2<\infty$, $-\infty<\beta_3<\infty$, $\frac{n\pi}{3}\le\gamma\le\frac{(n+1)\pi}{3}$, $0\le\theta_1\le 2\pi$, $0\le\theta_2\le\pi$ and $0\le\theta_3<2\pi$ with the volume element $d\tau=\beta_2^4\beta_3^3|\sin 3\gamma|d\beta_2 d\beta_3 d\gamma d\theta_1\sin\theta_2 d\theta_2 d\theta_3$. Here $\beta_\lambda^2=\sum\beta_{\lambda\mu}\beta_{\lambda\mu}^*$ is the measure of nucleus deformation with multipolarity λ. Below we consider nuclei that are hard with respect to octupole transverse and hexadecapole vibrations. So the current version of soft-rotator model of OPTMAN takes into account the non-axial quadrupole, octupole and hexadecapole deformations, and β_2, β_3 and $\gamma-$vibrations with account of nuclear volume conservation.

By giving suitably an initial assignment of quantum numbers to low-lying levels, we can adjust the nuclear Hamiltonian parameters to describe low-lyinng experimental levels (usually first levels of 3-4 rotational bands plus levels of the first negative parity rotational band). Example of such level description for ^{28}Si is demonstrated in Fig. 1.

Multipoles of deformed nuclear potential, with evident dependencies of deformations, necessary to built coupling appear from deformed nuclear radii, is given as follows by considering $\sum_{\lambda\mu}\beta_{\lambda\mu}Y_{\lambda\mu}(\theta',\varphi')$ small

$$V(r,R(\theta',\varphi')) \;=\; V(r,R_i) \;+\; \sum_{t=1}^{\max}\left.\frac{\partial^t V}{\partial R^t}\right|_{R=R_i}\frac{R_i^t}{t!}\{\sum_{\lambda\mu}\beta_{\lambda\mu}Y_{\lambda\mu}(\theta',\varphi')\}^t.$$

The optical nuclear potential was taken to be a standard form:

$$\begin{aligned} V(r) \;&=\; -(V_R+iW_V)f_R(r)+i4W_Da_D\frac{d}{dr}f_D(r)+V_C(r) \\ &\quad+\left(\frac{\hbar}{\mu_\pi c}\right)^2(V_{SO}+iW_{SO})\,\frac{1}{r}\frac{d}{dr}f_{SO}(r)\boldsymbol{\sigma}\cdot\mathbf{L} \end{aligned}$$

with the form factors given as

$$f_i=\left[1+\exp\left(r-R_i\right)/a_i\right]^{-1}, \qquad R_i \;=\; r_iA^{1/3}.$$

The symbols $i=R,V,D$ and *so* denote the real volume, imaginary volume, imaginary surface and spin-orbit potentials respectively. One can see, that imaginary volume and imaginary surface potential form factors were considered to be equal.

In case of expansion of Coulomb potential $V_C(r)$ with evident dependences on deformations, necessary to account deformations dynamics, we follow the suggestion of Satchler *et al.* [10], using a multipole expansion of the Coulomb potential $V_C(r)$ for charged ellipsoid with a uniform charge density within the Coulomb radius R_C and zero outside with some modifications (see [7, 11]).

In the mean time, energy dependence of the optical potential has been continuously improved guided by physical principles. Now, such features as the high-energy saturation behavior consistent with Dirac phenomenology, relativistic generalization of Elton and Madland, and properties stemming from the nuclear matter theory are taken into consideration[12].

$$\begin{aligned} V_R \;&=\; (V_R^0+V_R^1E^*+V_R^2E^{*2}+V_R^{DISP}e^{-\lambda_RE^*})\left[1+\frac{(-1)^{Z'+1}}{V_R^0+V_R^{DISP}}C_{viso}\frac{A-2Z}{A}\right] \\ &\quad+C_c\frac{ZZ'}{A^{1/3}}\varphi_c(E^*), \\ W_D \;&=\; \left[W_D^{DISP}+(-1)^{Z'+1}C_{wiso}\frac{A-2Z}{A}\right]e^{-\lambda_DE^*}\frac{E^{*2}}{E^{*2}+WID_D^2}, \\ W_V \;&=\; W_V^{DISP}\frac{E^{*2}}{E^{*2}+WID_V^2}, \\ V_{SO} \;&=\; V_{SO}^0e^{-\lambda_{so}E^*}, \\ W_{SO} \;&=\; W_{SO}^{DISP}\frac{E^{*2}}{E^{*2}+WID_{SO}^2}. \end{aligned}$$

Here, $E^*=(E_p-E_{fm})$, with E_p - energy of the projectile and E_{fm} - the Fermi energy, determined as $E_{fm}(Z,A)=-\frac{1}{2}\left[S_n(Z,A)+S_n(Z,A+1)\right]$ for neutrons and $E_{fm}(Z,A)=-\frac{1}{2}\left[S_p(Z,A)+S_p(Z+1,A+1)\right]$ for protons, where $S_i(Z,A)$ denotes the separation energy of nucleon i from a nucleus labeled by Z and A, while Z', Z and A are charges of incident particle, nucleus and nucleus mass number, respectively. As we intend to analyze neutron and

proton scattering data simultaneously, we want to have a unique optical potential for nucleons with form suggested by [12] with a term $C_c ZZ'/A^{1/3} \cdot \varphi_c(E^*)$ describing the Coulomb correction to the real optical potential and isospin terms $(-1)^{Z'+1} C_{viso}(A-2Z)/A \cdot \varphi_{viso}(E^*)$ and $(-1)^{Z'+1} C_{wiso}(A-2Z)/A \cdot \varphi_{wiso}(E^*)$. We assumed that energy dependencies of $\varphi_{viso}(E^*)$ and $\varphi_{wiso}(E^*)$ are the same as those of real and imaginary surface potentials, while $\varphi_c(E^*)$ were considered to be the minus derivative of real potential , so that

$$\varphi_c(E^*) \;=\; (\lambda_R V_R^{DISP} e^{-\lambda_R E^*} - V_R^1 - 2V_R^2 E^*) \left[1 + \frac{(-1)^{Z'+1}}{V_R^0 + V_R^{DISP}} C_{viso} \frac{A-2Z}{A} \right].$$

All the parameters were taken to be equal for neutrons and protons. We assume that Lane model [13] works, therefore the neutron-proton optical potential difference of the suggested potential stems from the isospin terms, the Coulomb correction terms and difference of the neutron-proton Fermi energies.

Calculations with OPTMAN are now possible both for neutrons and protons as the projectile, and the upper incident nucleon energy is extended to at least 200 MeV[14]. We couple all the levels considered not only with the ground state level, but between each other as it is shown on Fig. 2 for ^{28}Si case. With this options, OPTMAN is able to analyze the collective level structure, E2, E3, E4 $\gamma-$transition probabilities and reaction data in a self-consistent manner, which makes results of such analyses more reliable. We have found that this model was flexible enough so that OPTMAN can be applied not only to heavy rotational (actined) nuclei[15, 16], but can be applied very successfully even to a very light nucleus, namely ^{12}C[17, 18] and light one ^{28}Si[19], and also to vibrational nuclei such as ^{52}Cr[20], ^{56}Fe[21], ^{58}Ni[22].

3. Global Optical Potential Global Search for A=24-122 mass region

As we can account most strongly coupled levels in our CC calculations (we call such approach as a CC with saturated coupling), our best-fit OMPs are free of errors arising from unaccount of coupling in spherical case or lack of such coupling in case of standard rotator or vibrator model is used. Thus, as we get rid of the major nuclear collective structure effects in OMP now, we can expect to get global OMP systematics with a smooth dependence of OMP on the mass number.

As the first step to carry out CC optical model calculations, we adjusted soft-rotator nuclear Hamiltonian parameters to describe experimentally observed low-lying collective levels of ^{24,26}Mg, ^{28,30}Si, ^{32}S, ^{40}Ar, ^{40}Ca, ^{48}Ti, ^{52}Cr, ^{54,56}Fe, ^{58,60,62}Ni, ^{90,92}Zr, ^{92,94,94,98}Mo, ^{116,118,120,122}Sn nuclides, by considering levels with quantum numbers n_{β_2}=0, n_γ=0, K=0^+(G.S. band); n_{β_2}=0, n_γ=0, K=2^+; n_{β_2}=1, n_γ=0, K=0^+ and n_{β_2}=0, n_γ=0, K=0^- negative parity bands. Usually we coupled first 6-8 most strongly coupled collective levels. Nuclear wave functions with adjusted nuclear Hamiltonian parameters were used to built realistic coupling for coupled-channels calculations The best fit OMP for individual nuclides considered were found using a search option of OPTMAN code [7, 11] by minimizing the quantity χ^2, incorporating neutron total σ_{tot}, proton reaction cross-sections σ_{reac}, and elastic and inelastic angular distributions. All these available experimental observables, if any, were included in χ^2 search criteria. Smooth dependence of OMP for individual nuclides allowed to obtain a global OMP systematics, which is shown in Table 1. Overall χ^2 for all nuclides considered was found to be about 8, the main contribution to χ^2 came from excited levels other than the first 2_1^+ one. For total, elastic scattering and angular distributions with the first excited level excitation, it was usually less than 3.

Figure 3 demonstrates the quality of neutron total and proton nonelastic cross section predictions. One can see that we face no problems in describing total cross sections, as well as proton reaction cross sections. Fig. 4 shows the angular distributions of the neutron elastic

$V_R^0 = -35.93 - 0.025A$	$V_R^{DISP} = 94.88$
$\lambda_R = 0.004283$	
$V_R^1 = 0.03$	$V_R^2 = 0.00018$
$W_D^{DISP} = 21.11 - 37.68A^{-1/3}$	$\lambda_D = 0.0176$
$WID_D = 11.60$	
$W_V^{DISP} = 15.89$	$WID_V = 68.54 + 0.087A$
$V_{so}^0 = 5.922 + 0.003A$	$\lambda_{so} = 0.005$
$W_{SO}^{DISP} = -3.1$	$WID_{SO} = 160.00$
$r_R = 1.2450 - 0.2546A^{-1/3}$	$a_R = 0.683 - 0.132A^{-1/3}$
$r_D = 1.4217 - 0.5505A^{-1/3}$	$a_D = 0.536 - 0.059A^{-1/3}$
$r_C = 1.2607$	$a_C = 0.360$
$C_c = 0.9$	
$C_{viso} = 12.0$	$C_{wiso} = 14.00$
$r_{so} = 1.18 - 0.65A^{-1/3}$	$a_{so} = 0.59$

Table 1: The optical potential parameters for $24 \leq A \leq 122$ allowing the best fit of experimental data. Potential strengths in MeV; radii and diffusenesses in fm. (*Note that optical potential strengths except for the spin-orbit and Coulomb terms must be multiplied by a factor $K(E) = 2E/(E + M_pc^2)$ due to the relativistic generalization, see: Ref. [7, 11].)

scattering for ^{56}Fe and the proton elastic scattering for ^{90}Zr. Fig. 5 shows the angular distributions for the proton inelastic scattering leading to the first 2_1^+ level excitation of ^{28}Si and to the negative parity 3_1^- level excitation of ^{54}Fe. Angular distributions for these levels are described by our model with high accuracy for all nuclides considered. Analogous or a little worse quality is for angular distributions with the first 4_1^+ or the second 0_2^+ level excitation predictions. Fig. 6 shows prediction of neutron angular distributions for the excitation of the groups of the levels for ^{32}S and ^{92}Zr.

Finally in Fig. 7 we demonstrate predicted inelastic scattering angular distributions for ^{24}Mg and ^{122}Sn nuclides, which have the lightest and the heaviest mass among the considered by our global potential search.

Calculations shown in the figures were carried out with deformations equal for neutrons and protons, while we found that for single-closed-shell nuclei: ^{52}Cr, ^{54}Fe, ^{58,60,62}Ni, ^{92}Zr, ^{92}Mo and ^{116,118,120,122}Sn, deformations allowing best fit are greater for the probe for which the corresponding shell of the interacting nuclei is closed. Account of difference of the deformation parameters for incident neutron and proton may improve χ^2 by about 30%. This feature is consistent with the nuclear theory predictions [23].

4. Conclusion

We developed CC code OPTMAN within Soft-rotator nuclear model CC approach, allowing to analyze the collective level structure, E2, E3, E4 $\gamma-$transition probabilities and reaction data in a self-consistent manner. We have found that this model was flexible enough so that OPTMAN can be applied not only to heavy(actinide) nuclei, but can be applied very successfully even to a very light nucleus, and also medium weight vibrational nuclei.

Global optical potential for even-even nuclides in A=24 - 122 mass region is suggested. Expanding below A=24 and above A=122 is in progress

Acknowledgments

The authors are grateful to the guidance of late Dr. Y. Kikuchi, who started the collaboration among the authors and would like to thank the members of nuclear data groups at JIENR and JAERI for fruitful discussions and supports to this work.

A part of this work was supported through ISTC Project B-521, with Japan as Financing Party.

References

[1] A.I. Blokhin, A.V. Ignatjuk, V.N. Manokhin *et al.*, "BROND-2, Library of Recommended Evaluated Neutron Data, Documentation of Data Files", Yudernie Konstanty, issues 2+3 in English (1991).

[2] T. Tamura, Rev. Mod. Phys. **37**, 679 (1965).

[3] J. Raynal, "Optical Model and Coupled-Cannel Calculations in Nuclear Physics", IAEA SMR-9/8, IAEA (1970).

[4] Yu.V. Porodzinskiĭ and E.Sh. Sukhovitskiĭ, Phys. of Atom. Nucl. **59**, 247 (1996).

[5] Yu.V. Porodzinskiĭ and E.Sh. Sukhovitskiĭ, Sov. J. Nucl. Phys. **53**, 41 (1991).

[6] Yu.V. Porodzinskiĭ and E.Sh. Sukhovitskiĭ, Sov. J. Nucl. Phys. **54**, 570 (1991).

[7] E.Sh. Sukhovitskiĭ, Yu.V. Porodzinskiĭ, O. Iwamoto, S. Chiba and K. Shibata, JAERI-Data/Code 98-019 (1998); E.Sh. Soukhovitskiĭ, G.B. Morogovskiĭ, S. Chiba, O. Iwamoto, and T. Fukahori, JAERI-Data/Code 2004-002 (2004)

[8] A. Bohr and B.R. Mottelson, "Nuclear Structure, Vol. II, Nuclear Deformations", p.195, W. A. Benjamin Inc. (1975).

[9] A.S. Davydov, "Vozbuzhdennye sostoyaniya atomnykh yader (Excited States of Atomic Nuclei)", Moscow: Atomizdat (1969).

[10] R.H. Bassel, R.M. Drisko, and G.R. Satchler, Oak Ridge National Laboratory Report ORNL-3240, (1962).

[11] E.Sh. Sukhovitskiĭ, S. Chiba, J. Nucl. Sci.Technol. **Supple. 2**, 144-147 (2002).

[12] J.P. Delaroche, Y. Wang and J. Rapaport, Phys. ReV., **C39**, 391-404 (1989).

[13] A.M. Lane, Phys. Rev.Lett. **8**, 171-172 (1962); A.M. Lane, Nucl. Phys. **35**, 676-685, (1962).

[14] E.Sh. Soukhovitskiĭ and S. Chiba, J. Nucl. Sci. Technol. **Supple. 2**, 697(2002).

[15] E.Sh. Sukhovitskiĭ, O. Iwamoto, S. Chiba and T. Fukahori, J. Nucl. Sci. Technol. **37**, 120 (2000).

[16] E.Sh. Soukhovitski, S. Chiba, J. Nucl. Sci. Technol., **Supple. 2**, 144 (2002).

[17] S. Chiba, O. Iwamoto, Y. Yamanouti, M. Sugimoto, M. Mizumoto, K. Hasegawa, E.Sh. Sukhovitskiĭ, Yu. V. Porodzinskiĭ, and Y. Watanabe, Nucl. Phys. A **624**, 305 (1997).

[18] S. Chiba, O. Iwamoto, E.Sh. Sukhovitskiĭ, Yu. Watanabe and T. Fukahori, J. Nucl. Sci. Technol. **37**, 498 (2000).

[19] W. Sun, Y. Watanabe, E.Sh. Sukhovitskii, O. Iwamoto and S. Chiba, J. of Nucl. Sci. and Technol. **40**, 635 (2003).

[20] E.Sh. Sukhovitskiĭ, S. Chiba, J.-Y. Lee, B.-t. Kim and S.-W. Hong, J. Nucl. Sci. Technol. **40**, 69(2003).

[21] E. Sh. Sukhovitskiĭ, S. Chiba, J.-Y. Lee, Y.-O. Lee, J. Chang, T. Maruyama and O. Iwamoto, J. Nucl. Sci. Technol. **39**, 816 (2002); J.Y. Lee, E.Sh. Sukhovitskiĭ, Y.-O. Lee, J. Chang, S. Chiba and O. Iwamoto, J. Korean Phys. Soc. **38**, 88 (2001).

[22] E.Sh. Sukhovitskiĭ, Y.-O. Lee, J. Chang, S. Chiba and O. Iwamoto, Phys. Rev. **C62**, 044605 (2000).

[23] V.A. Madsen, V.R. Brown, J.D. Anderson, Phys Rev. **C12**, 1205-1211 (1975).

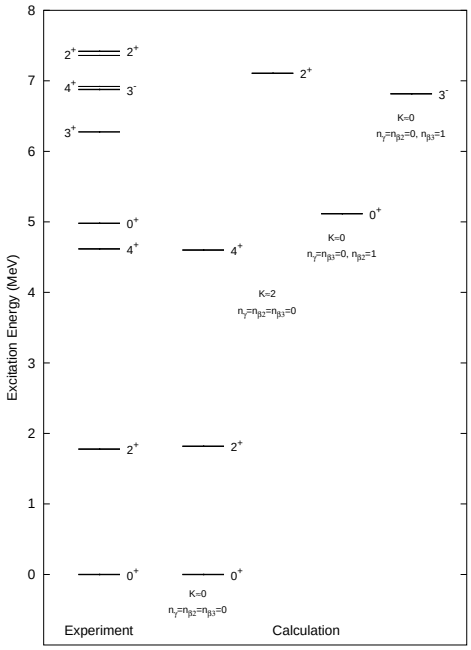

Figure 1: Comparison of the experimental and calculated ^{28}Si level schemes. Thick lines show experimental levels described by the soft rotator model.

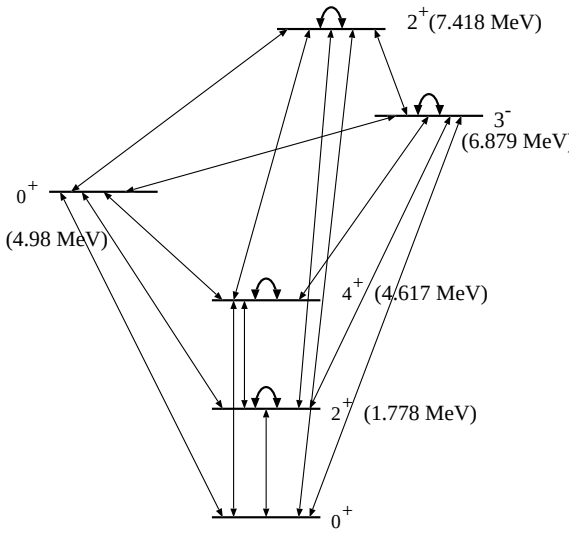

Figure 2: Coupling scheme employed in the present calculations for ^{28}Si. Arrows show the coupling used in the parameter search procedure.

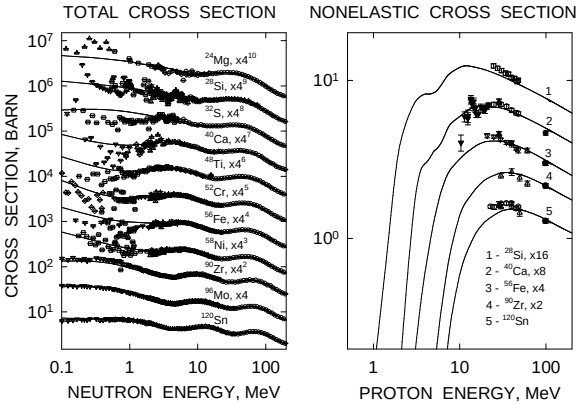

Figure 3: Comparison of neutron total and proton nonelastic cross sections: Predictions with the present global potential (solid lines), available experimental data (symbols).

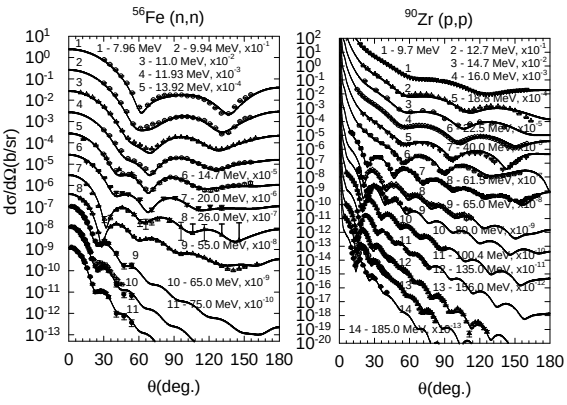

Figure 4: Comparison of experimental and predicted angular distributions of neutron elastic scattering for ^{56}Fe (left) and proton elastic for ^{90}Zr (right).

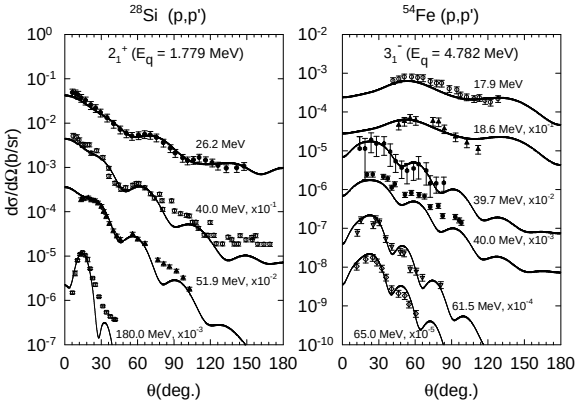

Figure 5: Comparison of experimental and predicted proton inelastic scattering angular distributions for excitation of the 2_1^+ level of ^{28}Si (left) and 3_1^- level of ^{54}Fe (right).

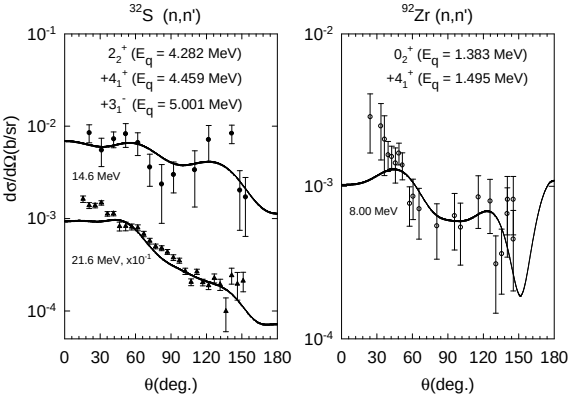

Figure 6: Comparison of experimental and predicted neutron angular distributions for excitations of groups of levels of ^{32}S (left) and ^{92}Zr (right).

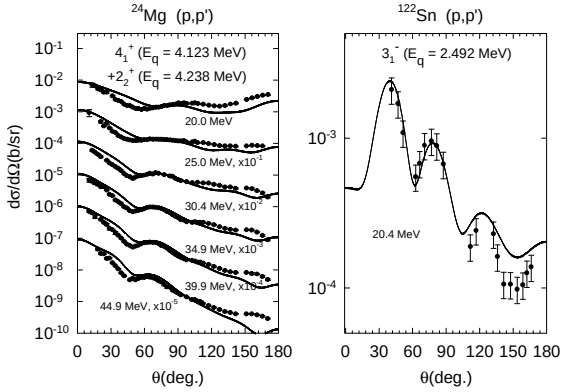

Figure 7: Comparison of experimental and predicted proton angular distributions for excitations of different levels of ^{24}Mg (left) and ^{122}Sn (right).